Image quality enhancement of computational integral imaging reconstruction for partially occluded objects using binary weighting mask on occlusion areas

Joon-Jae Lee,[1] Byung-Gook Lee,[2] and Hoon Yoo[3,*]

[1]Department of Game Mobile Contents, Keimyung University, Daemyung3-Dong Nam-Gu, Daegu 705-701, Korea

[2]Department of Visual Content, Dongseo University, San69-1, Jurye2-Dong, Sasang-Gu, Busan 617-716, Korea

[3]Division of Digital Media Technology, Sangmyung University, 7 Hongji-Dong, Jongro-Gu, Seoul 110-743, Korea

*Corresponding author: hunie@smu.ac.kr

Received 19 November 2010; revised 11 February 2011; accepted 11 February 2011; posted 15 March 2011 (Doc. ID 138456); published 28 April 2011

This paper presents an image quality enhancement of computational integral imaging reconstruction (CIIR) method by using a binary weighting mask on occlusion areas in elemental images. The proposed method utilizes a block-matching algorithm to estimate the occlusion areas in elemental images. Then, a binary weighting mask generated from the estimated occlusion area is applied to our CIIR method. This minimizes the overlapping effect of occluding objects in the reconstructed plane images and thus improves visual quality dramatically. To show the usefulness of our proposed scheme, we conduct several experiments and present the results. The experimental results indicate that our method is superior to the existing methods. © 2011 Optical Society of America

OCIS codes: 100.6890, 110.1758.

1. Introduction

In recent years, computational integral imaging [1–6] has been a good solution to overcome the challenging problems in partially occluded three-dimensional (3D) object recognition [7–10]. The approach uses two different processes: optical pickup, and computational integral imaging reconstruction (CIIR) based on the pinhole-array model. In the optical pickup process, a partially occluded 3D object is recorded by a lenslet array and a recording sensor to produce what are termed elemental images. In each elemental image, the 3D object is also partially occluded. In the CIIR process, the recorded elemental images are digitally reconstructed by using a computer where 3D images can be reconstructed at any distance. Since the occlusion hides the 3D object in elemental images, it seriously degrades the resolution of reconstructed images. That is, the unwanted images of the occlusion are overlapped into the plane images of the 3D object. Therefore, minimizing the unwanted noise image generated from the occlusion has the potential to improve the reconstructed 3D plane images in the CIIR method.

In this paper, to minimize the effect of occlusion, we propose an image quality enhancement method for a partially occluded 3D object by using a binary weighting mask on occlusion areas in elemental images. A 3D object is recorded as elemental images where it is partially occluded. Using the recorded elemental images, we first estimate the area of occlusion in the recorded elemental images by using a block-matching algorithm. Then, a binary weighting mask generated from the estimated occlusion area is applied to the CIIR method. The use of the proposed weighting mask can avoid the overlapping of

0003-6935/11/131889-05$15.00/0

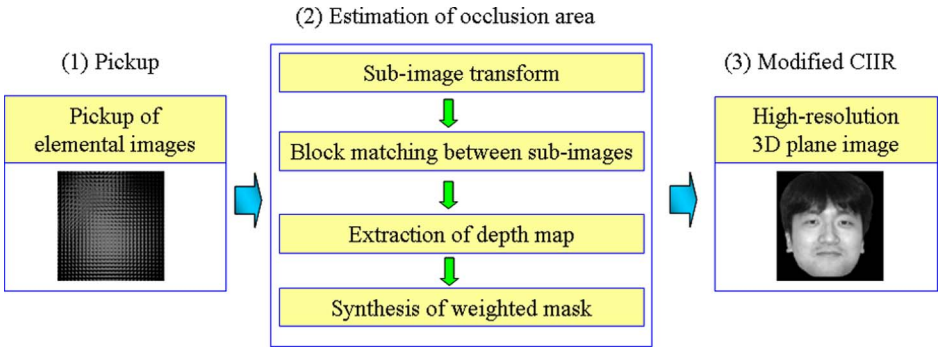

Fig. 1. (Color online) Diagram of the proposed scheme.

occlusion in the reconstructed plane images and the number of overlapping image can be changed for image normalization to find the exact mean images. Since we generate plane images from only the 3D object in elemental images, the visual quality can be improved dramatically. To show the usefulness of our proposed scheme, we carried out several experiments and present their results.

2. Proposed Method

The diagram of the proposed method is shown in Fig. 1. Our method consists of three different parts: pickup, estimation of occlusion areas, and a modified CIIR process.

A. Pickup of Elemental Images

Figure 2(a) shows the pickup process for a partially occluded 3D object. An occluding object and a 3D object of interest are located at two arbitrary distances z_o and z_r, respectively. They are recorded as elemental images by using a CCD camera. Here, the distance between the lenslet array and the elemental image plane was 3 mm. The lenslet array with 30×30 lenslets is located at $z = 0$ mm. The focal length and the lateral size of each lenslet are 3 mm and 1.08 mm, respectively. The resolution of the recorded elemental images is given by 900×900 because the resolution of each lenslet is 30×30 pixels. The recorded elemental images are shown in Fig. 2(b).

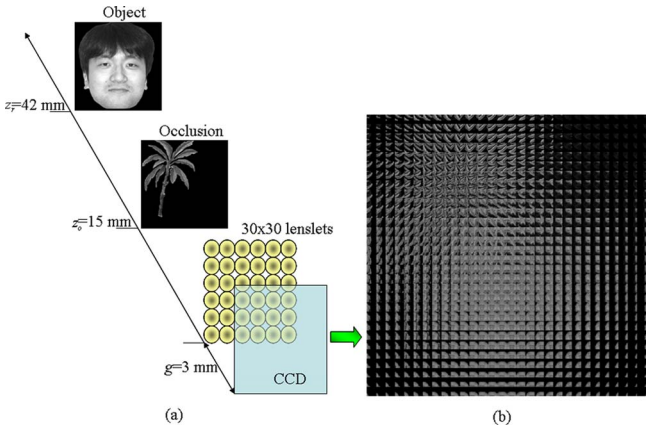

Fig. 2. (Color online) (a) Experimental setup for pickup process. (b) The recorded elemental images.

B. Estimation of Occlusion Area

The next step of the proposed method is estimation of occlusion areas in the recorded elemental images. To estimate the occlusion areas, we can use various 3D depth extraction methods [9–13]. In a previous work, we proposed a depth extraction method using the subimage transform and the stereo matching algorithm [9]. There, the elemental images were transformed into a subimage array. Then, a depth map for occlusion and a 3D object was calculated by using the block-matching algorithm. This method was able to remove occlusion areas easily and precisely. In the current paper, the previous method was used to estimate occlusion areas. The principle of our estimation of occlusion areas is shown in Fig. 3. We first perform a computational transform between the elemental image array and subimage array. In other words, the same position pixels for all elemental images are extracted and a collection of pixels with the same position is obtained as a subimage array. Let us suppose that the number of pixels for each elemental image is $s \times s$ and the number of elemental image is $l \times l$, respectively. The elemental image array E have become $(n \times n) = (sl \times sl)$ pixels. If $(m \times m)$ pixels are collected, the subimage array S is given by

$$S(i,j) = E(t_x s + q_x m + r_x, t_y s + q_y m + r_y), \quad (1)$$

where $q_x = [i/(ml)]$, $q_y = [j/(ml)]$, $p_x = i\%(ml)$, $p_y = j\%(ml)$, $t_x = [p_x/m]$, $t_y = [p_y/m]$, $r_x = i\%m$ and $r_y = j\%m$. $[x]$ is the largest integer less than or equal to the number x, and $a\%b$ is the reminder of a

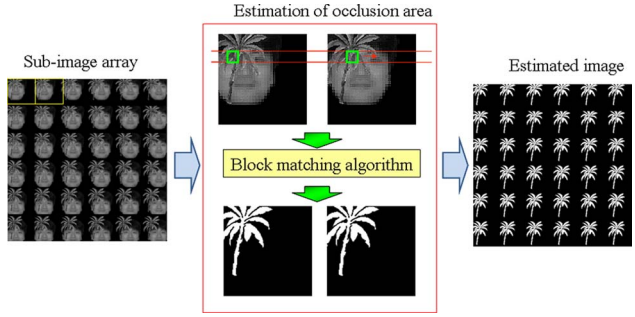

Fig. 3. (Color online) Conceptual diagram for estimation of occlusion area.

division by b. The subimage array transformed with Eq. (1) is shown on the left side of Fig. 3. The 5×5 pixels are collected from all elemental images.

Next, the block-matching algorithm is applied to the subimage array to find occlusion areas. We selected two adjacent subimages in the subimage array and applied a stereo block-matching algorithm [9] to two selective images. In the block-matching algorithm, the matching error between the blocks at the position (x,y) in the left image I_L and the candidate block at position $(x+u, y+v)$ in the reference image I_R is calculated. This is given by the sum of absolute difference (SAD),

$$\mathrm{SAD}_{(x,y)}(u,v) = \sum_{i=1}^{B}\sum_{j=1}^{B} |I_L(x+i,y+j) - I_R(x+u+i,y+v+j)|, \quad (2)$$

where the block size is $B \times B$. Using SAD results, we can find the best estimate $(\hat{u},\hat{v})$ value where SAD is minimized. This can be mathematically formulated as

$$(\hat{u},\hat{v}) = \mathrm{argmin}\,\mathrm{SAD}_{(x,y)}(u,v). \quad (3)$$

The depth map is calculated easily by the best estimate values. Based on the extracted depth map, we can estimate the position of occlusion [9].

After this process is repeated for all the subimages, we obtain a new subimage array for estimated occlusion areas, shown on the right side of Fig. 3. Finally, the elemental images for the occlusion areas are obtained by the inverse subimage transform. This is known as the binary weighting mask because it will be used for weighting values of 1 or 0 in the modified CIIR method.

C. Modified CIIR Method

In general, a CIIR method for the elemental images reconstructs a series of two-dimensional (2D) plane images volumetrically. In this paper, we apply both the original elemental images and the estimated binary weighting mask to the newly modified CIIR method.

Figure 4 shows the fundamental principle of our CIIR method, using both the original elemental images and the binary weighting mask. Let $I(x)$ be the intensity value of x at the distance z and n be the index of the corresponding elemental image. As shown in Fig. 4, $I(x)$ is evaluated from a set of pixels. It is determined by averaging the intensity value of all corresponding rays through the ray mapping, as shown in Fig. 4. However, since the binary weighting mask was obtained from the location where occlusion exists in the elemental images, we can use it to minimize the overlapping effect of occlusion. Therefore, we introduce a binary weighting mask $w_i(x)$ in the proposed CIIR method. That is, if a pixel in the elemental images is included within an occlusion area S, the binary weighting mask becomes zero,

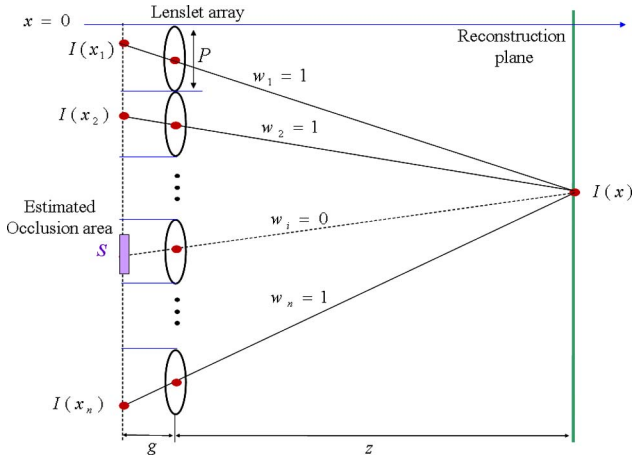

Fig. 4. (Color online) Principle of modified CIIR method.

as shown in Fig. 4. This means that the pixel within an occlusion area is excluded in calculation of a plane image. On the other hand, the pixels outside an occlusion area S are summated at the reconstruction plane. Then, our CIIR process is given by

$$I(x) = \frac{1}{N(x)}\sum_{i=1}^{n} w_i(x) I(x_i) = \frac{1}{N(x)}\sum_{i=1}^{n} w_i(x) I\left(-\frac{g}{z}x + P\left(i-\frac{1}{2}\right)\right), \quad (4)$$

where

$$w_i(x) = \begin{cases} 1, & P(i-1) \le x_i < Pi, x_i \in S \\ 0, & \text{elsewhere} \end{cases} \quad (5)$$

and

$$N(x) = \sum_{i=1}^{n} w_i(x). \quad (6)$$

Our CIIR method based on Eqs. (4)–(6) reconstructs the high-quality plane images because it reduces many unwanted noises generated by occlusion.

3. Experimental Results

To show the usefulness of the proposed technique, we performed computational experiments. The experimental structure is shown in Fig. 2. The "tree" image shown in Fig. 5(a) is used as an unknown occluding object located at $z_o = 15\,\mathrm{mm}$ from the lenslet array.

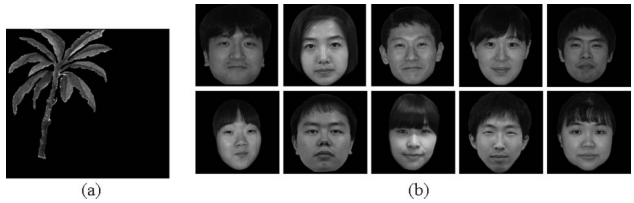

Fig. 5. (a) Occlusion. (b) Ten facial images.

The target objects to be recognized are ten "face" images that are located at $z_r = 42$ mm.

First, we recorded the elemental images for the occluding object and a target object. The lenslet array consists of 30 × 30 lenslets and the lenslet diameter is 1.08 mm. From this lenslet array, we obtained the elemental images with the resolution of 900 × 900 pixels as shown in Fig. 2(b). To estimate the area of occlusion, the recorded elemental images were transformed into the corresponding subimages which consist of 6 × 6 subimages, as shown in Fig. 3, left side. We applied the block matching to two subimages to obtain the depth information. In the extracted depth map, we can estimate occlusion areas because the occlusion is in front of the target object. We obtained the occlusion area subimages by repeating all subimages, as shown in Fig. 3, right side. Finally, they were transformed inversely into the occlusion area elemental images. These elemental images were used as the binary weighting mask in the modified CIIR process.

Using the original elemental images and the binary weighting mask, we carried out 3D image reconstruction experiments. The plane images for target objects Face 1 and Face 2 were reconstructed at 42 mm where the objects originally were located by using our CIIR method. The reconstructed images of the proposed method are shown in Fig. 6(d). For comparison, the facial images reconstructed in the conventional CIIR method [8] and the CIIR method with the occlusion removal technique [9] are shown in Figs. 6(b) and 6(c), respectively. As shown in Fig. 6(b), the image reconstructed from the conventional CIIR was blurred due to the overlapping unwanted image from the unknown occlusion. In the CIIR method with the occlusion removal technique, as shown in Fig. 6(c), the reconstructed image eliminated the unwanted occlusion image, but the result was not clear due to the use of the total number of overlapping image for all elemental images. However, it is seen that the blurring artifact is significantly reduced in the reconstructed images of the proposed CIIR method by using the binary weighting mask. This was because the binary weighting mask avoids the overlapping of occlusion in the reconstructed plane images and provides the number of overlapping images for only the 3D object in the elemental images in order to find the exact mean images.

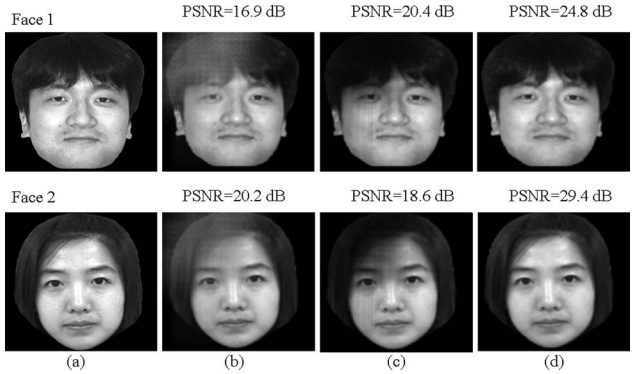

Fig. 6. For Face 1 and Face 2, (a) original images, (b) reconstructed plane image using the conventional CIIR method, (c) reconstructed plane image using the CIIR method with the previous occlusion removal technique, (d) reconstructed plane image using our modified CIIR method.

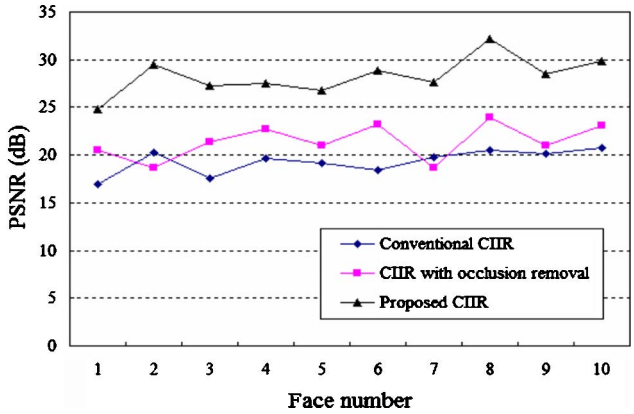

Fig. 7. (Color online) Graph of PSNR for ten test facial images.

To objectively evaluate our method, we calculated the peak signal-to-noise ratio (PSNR) for all test images. PSNR is defined as

$$\mathrm{PSNR}(I_o, I_r) = 10 \log_{10}\left(\frac{255^2}{\mathrm{MSE}(I_o, I_r)}\right), \qquad (7)$$

where I_o is the original image and I_r is the reconstructed image from a CIIR process. Mean squared error (MSE) is given by

$$\mathrm{MSE} = \frac{1}{pq}\sum_{x=0}^{p-1}\sum_{y=0}^{q-1}[I_o(x,y) - I_r(x,y)]^2, \qquad (8)$$

where x and y are the pixel coordinates of images having $p \times q$ pixels.

The PSNR results for ten facial images are presented in Fig. 7. Our proposed CIIR method was compared with the conventional CIIR method, and the CIIR method with the previous occlusion removal technique. We obtained a high improvement of 9 dB and 7 dB on average compared to the conventional CIIR method and the CIIR method with the previous occlusion removal method, respectively, in terms of PSNR from this experiment. The results in Fig. 7 show that our method is superior to the conventional methods in terms of visual quality.

4. Conclusion

We have proposed the modified CIIR method to obtain high-resolution plane images by reducing the overlapping of unwanted occlusion area images for a partially occluded object. The proposed method introduced the binary weighting mask based on the estimation of occlusion areas to minimize the overlapping effect of occlusion in the reconstruction plane. To show the usefulness of the proposed system, several experiments were performed and the

image quality improvement of 3D reconstructed images was demonstrated. The successful results showed the feasibility of the proposed system.

References

1. S.-H. Hong, J.-S. Jang, and B. Javidi, "Three-dimensional volumetric object reconstruction using computational integral imaging," Opt. Express **12**, 483–491 (2004).
2. D.-H. Shin, E.-S. Kim, and B. Lee, "Computational reconstruction technique of three-dimensional object in integral imaging using a lenslet array," Jpn. J. Appl. Phys. **44**, 8016–8018 (2005).
3. H. Yoo and D.-H. Shin, "Improved analysis on the signal property of computational integral imaging system," Opt. Express **15**, 14107–14114 (2007).
4. D.-H. Shin and E.-S. Kim, "Computational integral imaging reconstruction of 3D object using a depth conversion technique," J. Opt. Soc. Korea **12**, 131–135 (2008).
5. D.-C. Hwang, K.-J. Lee, S.-C. Kim, and E.-S. Kim, "Extraction of location coordinates of 3-D objects from computationally reconstructed integral images basing on a blur metric," Opt. Express **16**, 3623–3635 (2008).
6. D.-H. Shin and H. Yoo, "Scale-variant magnification for computational integral imaging and its application to 3D object correlator," Opt. Express **16**, 8855–8867 (2008).
7. B. Javidi, R. Ponce-Díaz, and S.-H. Hong, "Three-dimensional recognition of occluded objects by using computational integral imaging," Opt. Lett. **31**, 1106–1108 (2006).
8. S.-H. Hong and B. Javidi, "Distortion-tolerant 3D recognition of occluded objects using computational integral imaging," Opt. Express **14**, 12085–12095 (2006).
9. D.-H. Shin, B.-G. Lee, and J.-J. Lee, "Occlusion removal method of partially occluded 3D object using sub-image block matching in computational integral imaging," Opt. Express **16**, 16294–16304 (2008).
10. D.-H. Shin, H. Yoo, C.-W. Tan, B.-G. Lee, and J.-J. Lee, "Occlusion removal technique for improved recognition of partially occluded 3D objects in computational integral imaging," Opt. Commun. **281**, 4589–4597 (2008).
11. J.-H. Park, S. Jung, H. Choi, Y. Kim, and B. Lee, "Depth extraction by use of a rectangular lens array and one-dimensional elemental image modification," Appl. Opt. **43**, 4882–4895 (2004).
12. C. Wu, A. Aggoun, M. McCormick, and S. Y. Kung, "Depth extraction from unidirectional integral image using a modified multi-baseline technique," Proc. SPIE **4660**, 135–143 (2002).
13. J.-H. Park, G. Baasantseren, N. Kim, G. Park, J.-M. Kang, and B. Lee, "View image generation in perspective and orthographic projection geometry based on integral imaging," Opt. Express **16**, 8800–8813 (2008).